

Development of Advanced Operation Scenarios in Weak Magnetic-Shear Regime on JT-60U

T. Suzuki 1), N. Oyama 1), A. Isayama 1), Y. Sakamoto 1), T. Fujita 1), S. Ide 1), Y. Kamada 1), O. Naito 1), M. Sueoka 1), S. Moriyama 1), M. Hanada 1), and the JT-60 Team 1)

1) Japan Atomic Energy Agency, Naka, Ibaraki-ken, 311-0193 Japan

e-mail contact of main author: suzuki.takahiro@jaea.go.jp

Abstract. Fully non-inductive discharge having relaxed current profile and high bootstrap current fraction $f_{BS}=0.5$ has been realized in the high- β_p ELM My H-mode discharge with weak magnetic-shear satisfying $q_{95}=5.8$, $q_{min}=2.1$, and $q(0)=2.4$, where q_{min} and $q(0)$ are the safety factor q at the minimum and the plasma center, respectively. The rest of the plasma current is externally driven by neutral beams (NBs) and lower-hybrid (LH) waves. The safety factor profile evaluated by the motional Stark effect (MSE) diagnostic is kept unchanged during 0.7 s at the end of the full current drive (CD) sustainment for 2 s (1.5 times the current relaxation time). The loop voltage profile is spatially uniform at 0 V at the end of the sustainment. This demonstration contributes to the ITER steady-state operation scenario development. Another ITER advanced operation scenario, the hybrid operation scenario, has also been developed in the high- β_p ELM My H-mode with $q_{95}=3.2$ and $q_{min}\sim 1$. Period of sustainment at high $\beta_N=2.6$ has been almost tripled (to 28 s), and the JT-60U operation regime has extended toward longer sustainment and higher β_N . The development of advanced scenarios in JT-60U in these weak magnetic-shear regime leads development of advanced scenarios in ITER.

1. Introduction

Target of the JT-60U experimental program is to develop and establish advanced operation scenarios that support the forthcoming ITER operation, namely the steady-state operation scenario and the hybrid operation scenario. The steady-state (SS) operation requires full current drive condition (current drive fraction $f_{CD}=1$) that does not consume magnetic flux supplied from the Ohmic transformer coil (center solenoid in ITER). From the economic advantage, the SS operation also requires a high beta plasma having high bootstrap current fraction (f_{BS}) at reasonably low q_{95} . Since the bootstrap current in tokamak exists off-axis, it is considered that the plasma aiming at the SS operation will have broad or even hollow current profile, and hence flat or reversed magnetic-shear. Since strongly reversed shear plasma is not good at confining high-energy alpha particle produced by fusion reaction, flat or weakly reversed magnetic-shear regime (here we call weak magnetic-shear) is a promising candidate of the SS operation scenario. The high- β_p ELM My H-mode operation matches to this magnetic shear regime. Thus, development of the SS scenario is conducted in the high- β_p ELM My H-mode plasma. Another advanced operation scenario in ITER, that is the hybrid operation scenario, is to maximize the number of neutrons produced in a discharge. For that purpose, stable high beta operation at high plasma current (or low q_{95}) is required without a constraint of full CD.

Both of the scenarios are developed in the high- β_p ELM My H-mode regime with weak magnetic-shear that matches to large off-axis bootstrap current. Key issues in the steady-state operation are 1) fully non-inductive current drive ($f_{CD}=1$) at high bootstrap current fraction () and 2) fully relaxed current profile. In previous experiments [1,2], emphasis had been put on achievement of full-CD at higher I_p for larger fusion product ($3.1 \times 10^{20} \text{ m}^{-3} \text{ skeV}$) during relaxation of current profile. In this campaign, as shown in figure 1, JT-60U has successfully extended its operation regime reaching steady-state and full-CD at large f_{BS} , utilizing

combination of various current drivers.

Section 2 describes various current drivers in JT-60U that are used in this study. Development of steady state operation scenario is described in section 3. Section 4 gives development of long-pulse high-beta operation that contributes to the ITER hybrid operation scenario.

2. Current drivers in JT-60U

JT-60U is equipped with various current drivers, NBCD, LHCD, and ECCD. Here, current drivers used in this study (NBCD and LHCD) are briefly explained. JT-60U has 11 units of neutral beam injectors based on positive ion source (P-NBI [17]) and one unit of neutral beam injector

based on negative ion source (N-NBI [18]). Injection energies of the P-NBI and N-NBI are 80-85 keV and 320-360 keV, respectively. Injection powers of the P-NBI and N-NBI are 2-2.5 MW and 1-3 MW per NB unit, respectively. The injection energy and power depend on pulse length of injection. P-NBI and N-NBI have two ion sources in each unit. Figure 1 shows the poloidal cross section of JT-60U with NB trajectories. Two of 4 tangential P-NBIs are on-axis and the others are off-axis, in usual magnetic configuration in JT-60U. One of the two on-axis or two off-axis P-NBIs is injected to co-direction to the plasma current, and the others are to counter-direction for co/counter current drive, respectively. The other seven P-NBIs are injected almost perpendicular to the toroidal direction so that no effective NBCD is possible. Four of the seven P-NBIs injected from upper outboard are for on-axis heating, and the other three P-NBIs injected from lower outboard are for off-axis heating. N-NBI is tangentially injected almost on-axis to co-direction to the plasma current. Combination of these NBI systems enables us to realize various heating/current drive conditions, flexibly.

JT-60U is also equipped with the LHRF system at 2GHz. The antenna having the multi-junction structure [19] locates above the equatorial plane. Power of LH waves are about 1.5-2 MW in this campaign. The parallel refractive index N_{\parallel} of the primary component of the LH wave spectrum ranges 1.4-2.1, depending on the phase difference of the LH waves from two adjacent antenna modules. In order to obtain stable coupling of the LH waves, the gap between the plasma and the antenna front is controlled fixed during LHCD. The gap width is optimized with respect to better coupling and less heat load to the antenna from fast-ion bombardment.

3. Steady-state operation scenario in weak magnetic-shear regime

Two of the steady-state operation scenario was studied

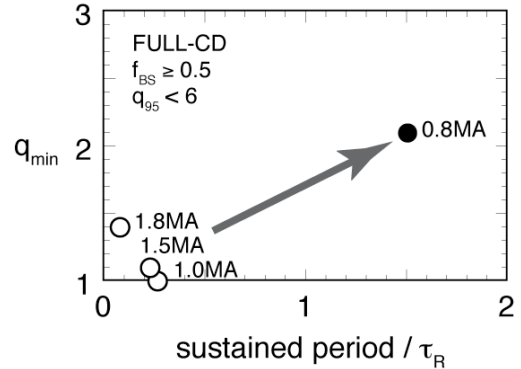


FIG. 1. Extended operation regime toward steady-state in weak magnetic-shear regime in this campaign (filled circles) from the previous ones (open circles). Shown are the discharges at full-CD with $f_{BS} \geq 0.5$ and $q_{min} < 6$.

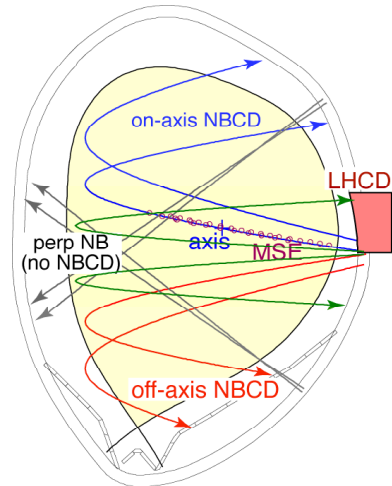


FIG. 2. Poloidal cross-section of the plasma and projection of trajectories of NBIs. Flexible use of on-/off-axis heating and current drive is possible in JT-60U. Location of LHRF antenna and measurement points of diagnostics are also indicated.

in this campaign, that is, NBCD scenario and LHCD scenario. The objective of the development of these steady state scenario is to establish the fully relaxed current profile under full CD in a high beta plasma having large bootstrap current fraction more than 50% at reasonably low $q_{95}\sim 5$ regime. Since the external current drive power is limited by the device condition, bootstrap current fraction, and hence, β_p should be raised to obtain full CD. The NBCD scenario raises β_p by creating internal transport barrier (ITB) via strong heating into a small volume plasma. The rest of the plasma current should be driven by the NBCD for full CD condition. In this small volume plasma, since the gap between the plasma and the LH antenna is large to couple LH waves into the plasma, LHCD cannot be used. On the other hand, LHCD scenario utilizes LHCD having high CD efficiency in addition to the NBCD and bootstrap current. In order to obtain good coupling of LH waves into the plasma, the gap between the plasma and antenna should be small, and hence, plasma volume should be large. This large volume condition becomes constraint to obtain high β_p since heating power density becomes low. In both scenarios, key issues are increasing bootstrap current fraction by obtaining strong ITB and H-mode edge for good confinement. If the plasma pressure p is the same, lower electron density n_e is preferable in order to increase external driven current ($\propto T_e/n_e \propto p/n_e^2$), while β_p and bootstrap fraction does not change. This also requires good confinement (as small NB heating power or as small NB fueling as possible).

3.1. NBCD scenario

Figure 3 shows one of good discharges in NBCD scenario developed in this campaign. In this discharge, plasma is initiated at $t=3$ s and plasma current ramp-up to 0.8MA continues until $t=5.5$ s. Toroidal magnetic field is 2.1T at geometric plasma center ($q_{95}=4.3$). During the I_p ramp-up, NB heating starts in order to prevent current penetration. During I_p flattop, main heating starts and plasma β is gradually increased along the feedback control of stored energy using control of NB heating power in order to prevent MHD activity. The reference value of the stored energy is kept constant (1.7MJ) after $t=8$ s, corresponding to $\beta_N=2.4$ and $\beta_p=1.8$ (FIG. 3(a)). About 4.0MW of co-tangential P-NB and 0.77MW ctr-tangential P-NB (for MSE diagnostics) is injected for NBCD in this discharge. In addition, 2.9MW of N-NB is injected after $t=7$ s (FIG. 3(b)). With the N-NB, surface loop voltage becomes close to zero (FIG. 3(c)). The loop voltage is defined by the time derivative of poloidal magnetic flux of equilibrium reconstructed using MSE diagnostics. The oscillation in the loop voltage is a result of slight β change around the reference value. Figure 4 shows radial profiles of safety factor, ion/electron temperatures and electron

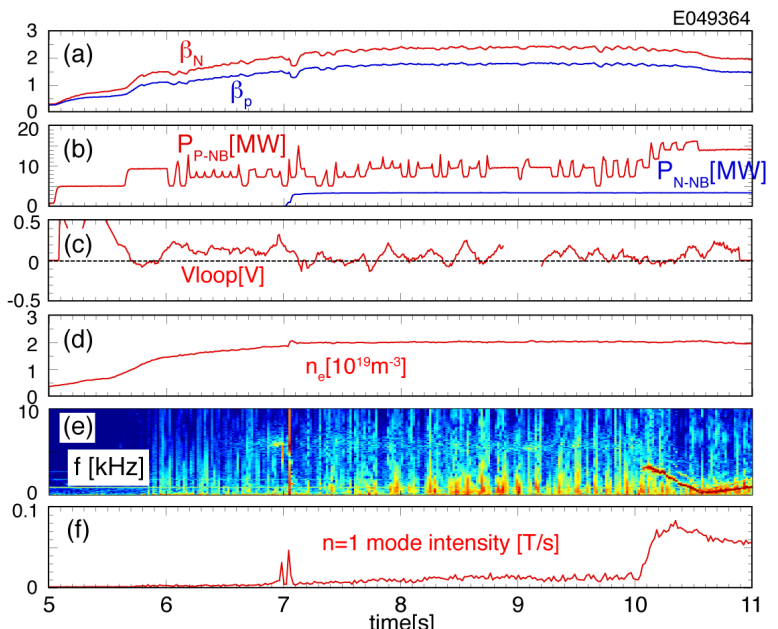


FIG. 3. Waveforms of (a) β_N (red) and β_p (blue), (b) heating power by P-NB (red) and N-NB (blue), surface loop voltage, (d) electron density, (e) spectrogram of magnetic fluctuation, and (f) magnetic fluctuation intensity of $n=1$ mode.

density at the start of constant β phase ($t=8$ s). Flat or weakly reversed magnetic shear structure is observed, where the minimum of q profile (q_{\min}) is about 1.7 at $r/a \sim 0.34$, and $q=2$ surface exists at $r/a \sim 0.6$. Clear ITB structure is observed in T_e , T_i and n_e , where the foot of the ITB locates around $r/a \sim 0.6$. While the temperature and density profiles are almost the same during the flattop phase of b ($t=8-10$ s), the q profile gradually changed and q_{\min} became lower due to the relaxation of toroidal electric field. With this change in q profile, r/a at $q=2$ surface became narrow and moved to steep pressure gradient region inside $r/a=0.6$, and then the $m/n=2/1$ mode terminated the high β phase at $t \sim 10$ s. Figure 4 (b) shows the T_i profile just before and after the mode. T_i became lower only inside the $q=2$ surface. This discharge clearly shows an importance of controlling q profile (especially location of low- q rational surface that is close to the steep pressure gradient region). This discharge also shows an importance of achieving fully relaxed current profile in the high b plasma, since a slight change in the q profile may cause an MHD activity. The decrease in q_{\min} or the shrink in $q=2$ surface is mainly caused by NBCD by N-NB, where the peak of NBCD profile locates at $r/a=0.2$. ACCOME code predicts bootstrap current and beam driven current are 0.41MA (52%) and 0.36MA (46%) where 0.18MA (23%) is driven by the N-NB. Current drive fraction was 97%.

3.2. LHCD scenario

Figure 3 shows the waveforms of the discharge during the flattop phase of plasma current ($I_p=0.8$ MA), toroidal field ($B_t=2.3$ T) and $q_{95}=5.8$. Pre-heating by counter-on-axis (for the MSE diagnostics) and co-off-axis NBs during I_p ramp-up produces the q profile with weak magnetic-shear, proceeded by strong NB heating at $t=5.2$ s in order to produce the internal transport barrier (ITB) and the ELM My H-mode edge. Then, the off-axis LHCD (wave frequency 2 GHz, parallel refractive index $N_{||}=1.9$ at 1.8 MW) and slightly off-axis N-NBCD (beam energy 320 keV at 1.2 MW) are applied after $t=6$ s to realize the full-CD and to sustain q profile and plasma pressure (or the bootstrap current); see figure 3 (a) and (b). As shown in figure 3 (c), the surface loop voltage (V_{loop}) stays about 0 V during $t=6.2-8.2$ s. Note that V_{loop} is determined by a linear fitting of poloidal magnetic flux within ± 0.1 s, so that the loop voltage starts increasing at $t=8.2$ s (0.1 s before the start of the notching of LH power due to arcing on antenna surface). The loop voltage inside the plasma becomes almost spatially uniform and 0 V at $t=8.2$ s at the end of the sustained period for 2 s corresponding to 1.5 times the current relaxation time (τ_R) given by [3]. Actually current profile at $t=7.5$ s and 8.0 s are almost identical, as shown in figure 3(d). The bootstrap current fraction is 50 %, and the external current driver drives the rest 50 % (26 % by off-axis LHCD and 24 % by on-axis NBCD) evaluated by the ACCOME code. With this scenario, the full-CD condition is

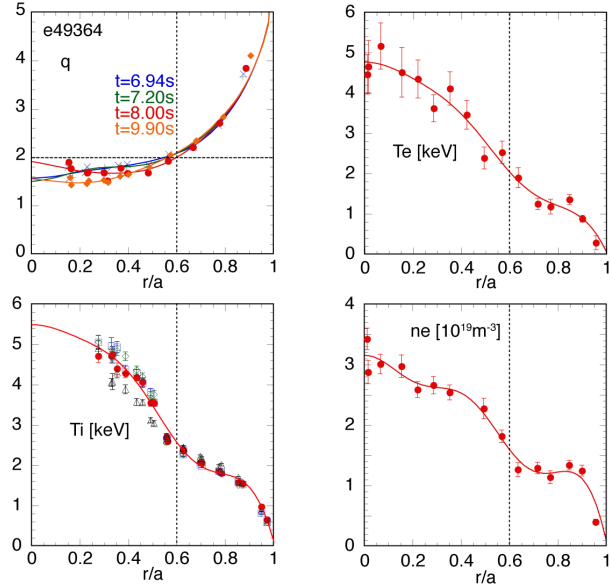


FIG. 4. (a) q profile at $t=6.94$ s, 7.2 s, 8.0 s, and 9.9 s, (b) ion temperature profile at $t=8.0$ s, 9.0 s, 9.97 s and 9.99 s, (c) electron temperature profile at $t=8.0$ s, electron density profile $t=8.0$ s in discharge shown in FIG. 3. Vertical dotted line shows $q=2$ surface location at $t=8.0$ s (start of flattop of β).

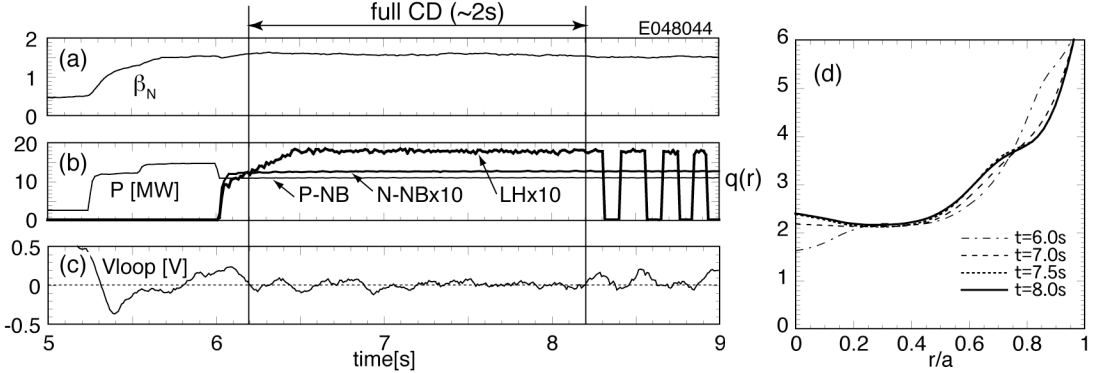


FIG. 5. Waveforms of (a) β_N , (b) injection power of P-NB (thin line), N-NB (medium line) and LH waves (thick line), (c) surface loop voltage. The full-CD condition lasts for about 2 s at fixed β_N . (d) safety factor profiles at $t=6.0$, 7.0 , 7.5 and 8.0 s measured by the MSE diagnostics. The safety factor profiles at $t=7.5$ and 8.0 s are almost identical so that current profile reached steady-state under full-CD. The q_{min} and the $q(0)$ at $t=8.0$ s are 2.1 and 2.4 , respectively.

maintained for about 2 s at constant β , until the notching of LH power starts at $t=8.3$ s. Therefore, the q profile at $t=8.0$ s shown in figure 3 (d) could have been maintained if current drive and heating continued.

In this discharge, no MHD activity, such as neo-classical tearing mode (NTM), is observed, since there is no low- q rational surface, e.g. 1, $3/2$ and 2, after $t=6.5$ s. Note that clear ITB structure is observed in Ti, Te, and ne (see FIG. 6), where these ITB contributes to enhance bootstrap current. Since the current profile reaches steady-state, we did not expect appearance of MHD due to the change in q profile as observed in the NBCD scenario. The achieved β ($\beta_N=1.6$, $\beta_p=1.5$) was limited by the H-mode pedestal density that permits access of LH waves into the core region (so-called wave accessibility condition). Electron density at the pedestal was $1.2 \times 10^{19} \text{ m}^{-3}$ in discharge shown in figure 3. When a larger NB heating power is injected for a higher β in similar discharges, increase in the pedestal density due to increased NB fueling leads to reduction of LHCD current and break of the full-CD condition. An increase in the bootstrap current at the higher β was not sufficient to compensate the reduction of LH driven current. Reduction of B_t in order to raise β_N has also resulted in a similar result.

In order to investigate the applicability of this weak magnetic-shear q profile to a further high β operation, behavior of this type of discharge with stronger ITB (and at higher β) was investigated, but without full-CD condition. Operation scenario is almost the same as the discharge shown in Fig. 5, however NB power (both P-NB and N-NB) is increased for higher β . In this discharge, an $n=1$ MHD occurs at $t \sim 9.4$ s. The safety factor and ion temperature profile before the MHD activity is shown in Fig. 7. In this discharge, ITB strength is gradually increasing (β_N reaches 2.1), and the foot of ITB is close to (or slightly inward than) the $q=3$ surface. When the $n=1$ MHD appears, Ti inside $q=3$ surface drops so that this mode is considered to be $m/n=3/1$ mode. This behavior of Ti is similar to the NBCD scenario (FIG. 4),

where the $q=2$ surface resonant to $m/n=2/1$ mode was in concern. Thus, this result again raises importance of controlling the location of rational surface if the rational surface is close to the steep pressure gradient region.

4. Extending operation regime toward long-pulse higher β_N for hybrid operation scenario

Another advanced operation scenario planned in ITER is the hybrid operation scenario, where the large current (low q_{95}) operation is required at high β_N and with a moderate CD fraction. JT-60U has extended the operation regime toward such longer pulse and higher β_N in order to contribute to the ITER hybrid scenario, making full use of the reinforced heating power for long pulse in this campaign; see figure 8. Power supply systems for 3 units of P-NBs (about 6 MW) are modified to enable 30 s operation (10 s formerly). The sustained period at $\beta_N=2.6$ has been almost tripled from 10 s to 28 s ($\sim 16\tau_R$) in the high- β_p ELM My H-mode plasma at low $q_{95}=3.2$ ($I_p=0.9$ MA, $B_t=1.5$ T). Good confinement ($H_{H98y} \geq 1$) is kept for 25 s, where the period is limited by the degradation of confinement (after $t=29$ s in figure 8(a)) due to increase in density caused by enhanced recycling. Figure 9 show the safety factor profile in this discharge, where flat q profile is observed inside $r/a=0.5$. In this discharge, off-axis bootstrap current ($f_{BS}=0.43$, $f_{CD}=0.48$) maintains the weak magnetic-shear at $q_{min} \sim 1$. Weak and infrequent sawtooth activity is observed which hardly affects the confinement. Due to the low $q_{95}=3.2$ and the flat q profile at the core region, rational surface at low- q ($m/n=3/2$, $2/1$, and $3/1$) exists outside the steep pressure gradient region (see FIG. 9).

Comparing the thermal pressure to that obtained in the last campaign ($\beta_N=2.3$), thermal pressure profile is more peaked in the core region ($r/a < 0.4$). The sustainment of this peaked pressure profile was enabled by the long pulse injection of P-NB, described above, having on-axis heating profile. This increase in core pressure contributed to

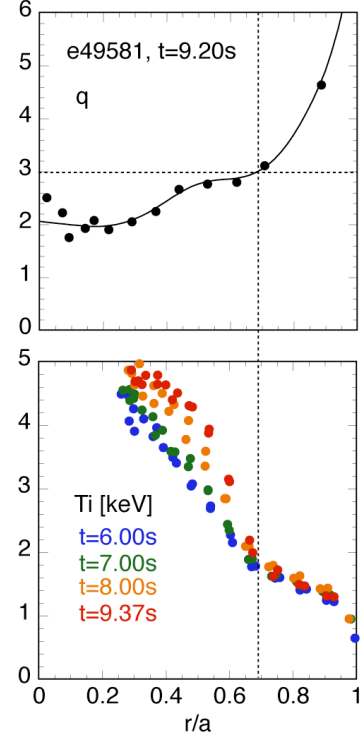


FIG. 7. q profile ($t=9.2$ s before MHD) and temporal evolution of T_i profiles at $t=6.0$, 7.0 , 8.0 , 9.37 (just before MHD) s.

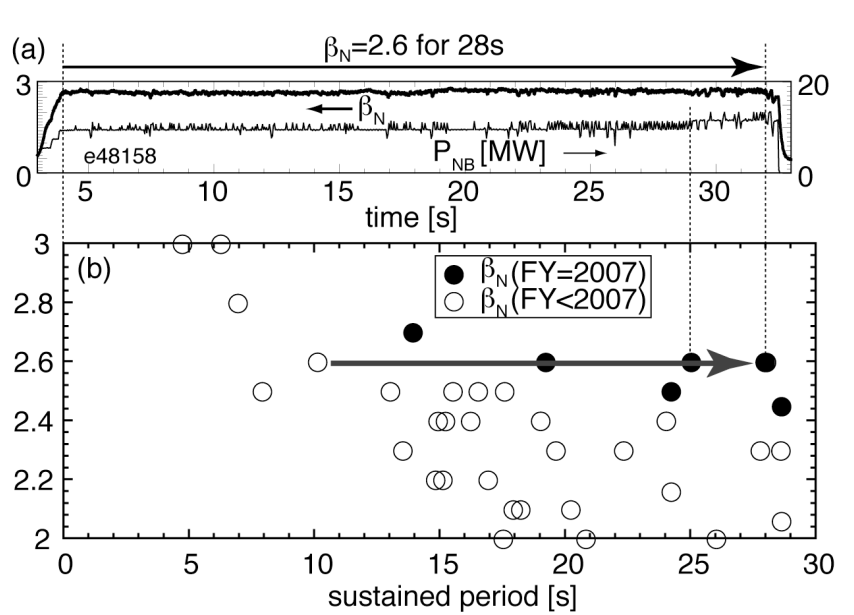


FIG. 8. (a) Waveforms of a discharge at $\beta_N=2.6$ sustained for 28 s (and $H_{H98y} \geq 1$ for 25 s). (b) Extended operation regime toward longer sustainment and higher $\beta_N H_{H98y}$ (filled circles) from previous campaigns [4] (open circles). Period of $\beta_N=2.6$ sustainment has been almost tripled.

raise β_N . Although the pressure gradient became steeper than the last campaign, this discharge was free from MHD activity related to this steep pressure gradient region. This q profile was quite effective to raise β_N with this centrally peaked pressure profile.

5. Summary

Fully non-inductive discharge having relaxed current profile and high bootstrap current fraction $f_{BS}=0.5$ has been realized in the high- β_p ELM My H-mode discharge ($\beta_N=1.6$, $\beta_p=1.5$) with weak magnetic-shear satisfying $q_{95}=5.8$, $q_{min}=2.1$, and $q(0)=2.4$. The rest of the plasma current is externally driven by NBs and LH waves. The safety factor profile is kept unchanged during 0.7 s at the end of the full CD sustainment for 2 s (1.5 times the current relaxation time). The loop voltage profile is spatially uniform at 0 V at the end of the sustainment. In addition, it was found that $m/n=3/1$ MHD that is resonant to the $q=3$ surface limits the β_N in this weak magnetic-shear scenario when the steep pressure gradient region exists at the $q=3$ surface. This demonstration contributes to the development and optimization of the ITER steady-state operation scenario. Another ITER advanced operation scenario, the hybrid operation scenario, has also been developed in the high- β_p ELM My H-mode with $q_{95}=3.2$ and $q_{min}\sim 1$. Period of sustainment at high $\beta_N=2.6$ has been almost tripled (to 28 s), and the JT-60U operation regime has extended toward longer sustainment and higher β_N . The development of advanced scenarios in JT-60U in these weak magnetic-shear regime contributes development of advanced scenarios in ITER.

Acknowledgements

The authors thank to the JT-60 team for cooperation in conducting this study.

References

- [1] KAMADA, Y., et al., Nucl. Fusion **41** (2001) 1311.
- [2] ISAYAMA, A., et al., Nucl. Fusion **43** (2003) 1272.
- [3] MIKKELSEN, D.R., Phys. Fluids **B1** (1989) 333.
- [4] OYAMA, N., et al., Nucl. Fusion. **47** (2007) 689.
- [5] SUZUKI, T., et al., Proceeding of 20th IAEA Conference (2004) IAEA-CN-116/EX/1-3.
- [6] OIKAWA, T., et al., Nucl. Fusion **40** (2000) 435.
- [7] OIKAWA, T., et al., Nucl. Fusion **41** (2001) 1575.
- [8] SUZUKI, T., et al., Plasma Phys. Control. Fusion **44** (2001) 1.
- [9] SUZUKI, T., et al., J. Plasma Fusion Res. **80** (2004) 511.
- [10] PETTY, C.C., et al., Nucl. Fusion **42** (2002) 1366.
- [11] PETTY, C.C., et al., Nucl. Fusion **43** (2003) 700.
- [12] FUJITA, T., et al., FT/P7-4, this conference.
- [13] IDE, S., et al., Phys. Rev. Lett. **73** (1994) 2312.
- [14] NAITO, O., et al., Phys. Rev. Lett. **89** (2002) 065001.

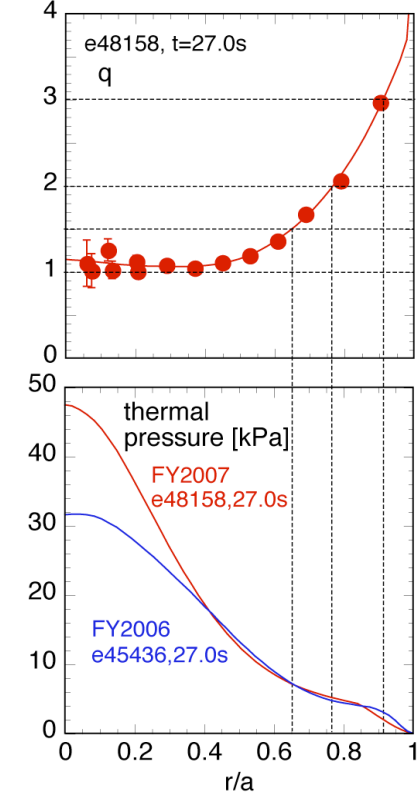


FIG. 9. Profiles of safety factor and thermal pressure at $t=27.0s$ in discharge shown in FIG. 8 ($\beta_N=2.6$, red). Thermal pressure profile in the last campaign $\beta_N=2.3$, blue) is also plotted.

- [15] SUZUKI, T., et al., J. Plasma Fusion Res. **80** (2004) 362.
- [16] FUJITA, T., et al., Fusion Eng. Des. **34-35** (1997) 289.
- [17] ISHIKAWA, M., et al., Rev. Sci. Instrum. **73** (2002) 4237.
- [18] KURIYAMA, M., et al., Fusion Sci. Tech. **42** (2002) 424.
- [19] KURIYAMA, M., et al., Fusion Sci. Tech. **42** (2002) 410.
- [20] SEKI, M., et al., Fusion Sci. Tech. **42** (2002) 452.
- [21] SEKI, M., et al., Fusion Eng. Des. **74** (2005) 273.
- [22] IDE, S., et al., Plasma Phys. Control. Fusion **44** (2002) L63.
- [23] SUZUKI, T., et al., Rev. Sci. Instrum. **77** (2006) 10E914.
- [24] FOREST, C.B., et al., Phys. Rev. Lett., **73** (1994) 2444.
- [25] TANI, K., et al., J. Computational Phys. **98** (1992) 332.